

**Observation of Hadronic W Decays
in $t\bar{t}$ Events with the Collider Detector at Fermilab**

Submitted to PRL

F. Abe,¹⁷ H. Akimoto,³⁹ A. Akopian,³¹ M. G. Albrow,⁷ A. Amadon,⁵ S. R. Amendolia,²⁷ D. Amidei,²⁰ J. Antos,³³ S. Aota,³⁷ G. Apollinari,³¹ T. Arisawa,³⁹ T. Asakawa,³⁷ W. Ashmanskas,¹⁸ M. Atac,⁷ P. Azzi-Bacchetta,²⁵ N. Bacchetta,²⁵ S. Bagdasarov,³¹ M. W. Bailey,²² P. de Barbaro,³⁰ A. Barbaro-Galtieri,¹⁸ V. E. Barnes,²⁹ B. A. Barnett,¹⁵ M. Barone,⁹ G. Bauer,¹⁹ T. Baumann,¹¹ F. Bedeschi,²⁷ S. Behrends,³ S. Belforte,²⁷ G. Bellettini,²⁷ J. Bellinger,⁴⁰ D. Benjamin,³⁵ J. Bensinger,³ A. Beretvas,⁷ J. P. Berge,⁷ J. Berryhill,⁵ S. Bertolucci,⁹ S. Bettelli,²⁷ B. Bevensee,²⁶ A. Bhatti,³¹ K. Biery,⁷ C. Bigongiari,²⁷ M. Binkley,⁷ D. Bisello,²⁵ R. E. Blair,¹ C. Blocker,³ S. Blusk,³⁰ A. Bodek,³⁰ W. Bokhari,²⁶ G. Bolla,²⁹ Y. Bonushkin,⁴ D. Bortoletto,²⁹ J. Boudreau,²⁸ L. Breccia,² C. Bromberg,²¹ N. Bruner,²² R. Brunetti,² E. Buckley-Geer,⁷ H. S. Budd,³⁰ K. Burkett,²⁰ G. Busetto,²⁵ A. Byon-Wagner,⁷ K. L. Byrum,¹ M. Campbell,²⁰ A. Caner,²⁷ W. Carithers,¹⁸ D. Carlsmith,⁴⁰ J. Cassada,³⁰ A. Castro,²⁵ D. Cauz,³⁶ A. Cerri,²⁷ P. S. Chang,³³ P. T. Chang,³³ H. Y. Chao,³³ J. Chapman,²⁰ M. -T. Cheng,³³ M. Chertok,³⁴ G. Chiarelli,²⁷ C. N. Chiou,³³ L. Christofek,¹³ M. L. Chu,³³ S. Cihangir,⁷ A. G. Clark,¹⁰ M. Cobal,²⁷ E. Cocca,²⁷ M. Contreras,⁵ J. Conway,³² J. Cooper,⁷ M. Cordelli,⁹ D. Costanzo,²⁷ C. Couyoumtzelis,¹⁰ D. Cronin-Hennessy,⁶ R. Culbertson,⁵ D. Dagenhart,³⁸ T. Daniels,¹⁹ F. DeJongh,⁷ S. Dell'Agnello,⁹ M. Dell'Orso,²⁷ R. Demina,⁷ L. Demortier,³¹ M. Deninno,² P. F. Derwent,⁷ T. Devlin,³² J. R. Dittmann,⁶ S. Donati,²⁷ J. Done,³⁴ T. Dorigo,²⁵ N. Eddy,²⁰ K. Einsweiler,¹⁸ J. E. Elias,⁷ R. Ely,¹⁸ E. Engels, Jr.,²⁸ D. Errede,¹³ S. Errede,¹³ Q. Fan,³⁰ R. G. Feild,⁴¹ Z. Feng,¹⁵ C. Ferretti,²⁷ I. Fiori,² B. Flaughier,⁷ G. W. Foster,⁷ M. Franklin,¹¹ J. Freeman,⁷ J. Friedman,¹⁹ H. Frisch,⁵ Y. Fukui,¹⁷ S. Galeotti,²⁷ M. Gallinaro,²⁶ O. Ganel,³⁵ M. Garcia-Sciveres,¹⁸ A. F. Garfinkel,²⁹ C. Gay,⁴¹ S. Geer,⁷ D. W. Gerdes,¹⁵ P. Giannetti,²⁷ N. Giokaris,³¹ P. Giromini,⁹ G. Giusti,²⁷ M. Gold,²² A. Gordon,¹¹ A. T. Goshaw,⁶ Y. Gotra,²⁵ K. Goulianos,³¹ H. Grassmann,³⁶ L. Groer,³² C. Grossos-Pilcher,⁵ G. Guillian,²⁰ J. Guimaraes da Costa,¹⁵ R. S. Guo,³³ C. Haber,¹⁸ E. Hafen,¹⁹ S. R. Hahn,⁷ R. Hamilton,¹¹ T. Handa,¹² R. Handler,⁴⁰ F. Happacher,⁹ K. Hara,³⁷ A. D. Hardman,²⁹ R. M. Harris,⁷ F. Hartmann,¹⁶ J. Hauser,⁴ E. Hayashi,³⁷ J. Heinrich,²⁶ W. Hao,³⁵ B. Hinrichsen,¹⁴ K. D. Hoffman,²⁹ M. Hohlmann,⁵ C. Holck,²⁶ R. Hollebeek,²⁶ L. Holloway,¹³ Z. Huang,²⁰ B. T. Huffman,²⁸ R. Hughes,²³ J. Huston,²¹ J. Huth,¹¹ H. Ikeda,³⁷ M. Incagli,²⁷ J. Incandela,⁷ G. Introzzi,²⁷ J. Iwai,³⁹ Y. Iwata,¹² E. James,²⁰ H. Jensen,⁷ U. Joshi,⁷ E. Kajfasz,²⁵ H. Kambara,¹⁰ T. Kamon,³⁴ T. Kaneko,³⁷ K. Karr,³⁸ H. Kasha,⁴¹ Y. Kato,²⁴ T. A. Keaffaber,²⁹ K. Kelley,¹⁹ R. D. Kennedy,⁷ R. Kephart,⁷ D. Kestenbaum,¹¹ D. Khazins,⁶ T. Kikuchi,³⁷ B. J. Kim,²⁷ H. S. Kim,¹⁴ S. H. Kim,³⁷ Y. K. Kim,¹⁸ L. Kirsch,³ S. Klimenko,⁸ D. Knoblauch,¹⁶ P. Koehn,²³ A. Konigeter,¹⁶ K. Kondo,³⁷ J. Konigsberg,⁸ K. Kordas,¹⁴ A. Korytov,⁸ E. Kovacs,¹ W. Kowald,⁶ J. Kroll,²⁶ M. Kruse,³⁰ S. E. Kuhlmann,¹ E. Kuns,³² K. Kurino,¹² T. Kuwabara,³⁷ A. T. Laasanen,²⁹ I. Nakano,¹² S. Lami,²⁷ S. Lammel,⁷ J. I. Lamoureux,³ M. Lancaster,¹⁸ M. Lanzoni,²⁷ G. Latino,²⁷ T. LeCompte,¹ S. Leone,²⁷ J. D. Lewis,⁷ P. Limon,⁷ M. Lindgren,⁴ T. M. Liss,¹³ J. B. Liu,³⁰ Y. C. Liu,³³ N. Lockyer,²⁶ O. Long,²⁶ C. Loomis,³² M. Loreti,²⁵ D. Lucchesi,²⁷ P. Lukens,⁷ S. Lusin,⁴⁰ J. Lys,¹⁸ K. Maeshima,⁷ P. Maksimovic,¹⁹ M. Mangano,²⁷ M. Mariotti,²⁵ J. P. Marriner,⁷ A. Martin,⁴¹ J. A. J. Matthews,²² P. Mazzanti,² P. McIntyre,³⁴ P. Melese,³¹ M. Menguzzato,²⁵ A. Menzione,²⁷ E. Meschi,²⁷ S. Metzler,²⁶ C. Miao,²⁰ T. Miao,⁷

G. Michail,¹¹ R. Miller,²¹ H. Minato,³⁷ S. Miscetti,⁹ M. Mishina,¹⁷ S. Miyashita,³⁷ N. Moggi,²⁷ E. Moore,²² Y. Morita,¹⁷ A. Mukherjee,⁷ T. Muller,¹⁶ P. Murat,²⁷ S. Murgia,²¹ H. Nakada,³⁷ I. Nakano,¹² C. Nelson,⁷ D. Neuberger,¹⁶ C. Newman-Holmes,⁷ C.-Y. P. Ngan,¹⁹ L. Nodulman,¹ S. H. Oh,⁶ T. Ohmoto,¹² T. Ohsugi,¹² R. Oishi,³⁷ M. Okabe,³⁷ T. Okusawa,²⁴ J. Olsen,⁴⁰ C. Pagliarone,²⁷ R. Paoletti,²⁷ V. Papadimitriou,³⁵ S. P. Pappas,⁴¹ N. Parashar,²⁷ A. Parri,⁹ J. Patrick,⁷ G. Pauletta,³⁶ M. Paulini,¹⁸ A. Perazzo,²⁷ L. Pescara,²⁵ M. D. Peters,¹⁸ T. J. Phillips,⁶ G. Piacentino,²⁷ M. Pillai,³⁰ K. T. Pitts,⁷ R. Plunkett,⁷ L. Pondrom,⁴⁰ J. Proudfoot,¹ F. Ptohos,¹¹ G. Punzi,²⁷ K. Ragan,¹⁴ D. Reher,¹⁸ M. Reischl,¹⁶ A. Ribon,²⁵ F. Rimondi,² L. Ristori,²⁷ W. J. Robertson,⁶ T. Rodrigo,²⁷ S. Rolli,³⁸ L. Rosenson,¹⁹ R. Roser,¹³ T. Saab,¹⁴ W. K. Sakumoto,³⁰ D. Saltzberg,⁴ A. Sansoni,⁹ L. Santi,³⁶ H. Sato,³⁷ P. Schlabach,⁷ E. E. Schmidt,⁷ M. P. Schmidt,⁴¹ A. Scott,⁴ A. Scribano,²⁷ S. Segler,⁷ S. Seidel,²² Y. Seiya,³⁷ F. Semeria,² T. Shah,¹⁹ M. D. Shapiro,¹⁸ N. M. Shaw,²⁹ P. F. Shepard,²⁸ T. Shibayama,³⁷ M. Shimojima,³⁷ M. Shochet,⁵ J. Siegrist,¹⁸ A. Sill,³⁵ P. Sinervo,¹⁴ P. Singh,¹³ K. Sliwa,³⁸ C. Smith,¹⁵ F. D. Snider,¹⁵ J. Spalding,⁷ T. Speer,¹⁰ P. Sphicas,¹⁹ F. Spinella,²⁷ M. Spiropulu,¹¹ L. Spiegel,⁷ L. Stanco,²⁵ J. Steele,⁴⁰ A. Stefanini,²⁷ R. Ströhmer,^{7a} J. Strologas,¹³ F. Strumia,¹⁰ D. Stuart,⁷ K. Sumorok,¹⁹ J. Suzuki,³⁷ T. Suzuki,³⁷ T. Takahashi,²⁴ T. Takano,²⁴ R. Takashima,¹² K. Takikawa,³⁷ M. Tanaka,³⁷ B. Tannenbaum,²² F. Tartarelli,²⁷ W. Taylor,¹⁴ M. Tecchio,²⁰ P. K. Teng,³³ Y. Teramoto,²⁴ K. Terashi,³⁷ S. Tether,¹⁹ D. Theriot,⁷ T. L. Thomas,²² R. Thurman-Keup,¹ M. Timko,³⁸ P. Tipton,³⁰ A. Titov,³¹ S. Tkaczyk,⁷ D. Toback,⁵ K. Tollefson,¹⁹ A. Tollestrup,⁷ H. Toyoda,²⁴ W. Trischuk,¹⁴ J. F. de Troconiz,¹¹ S. Truitt,²⁰ J. Tseng,¹⁹ N. Turini,²⁷ T. Uchida,³⁷ F. Ukegawa,²⁶ S. C. van den Brink,²⁸ S. Vejcik, III,²⁰ G. Velev,²⁷ R. Vidal,⁷ R. Vilar,^{7a} D. Vucinic,¹⁹ R. G. Wagner,¹ R. L. Wagner,⁷ J. Wahl,⁵ N. B. Wallace,²⁷ A. M. Walsh,³² C. Wang,⁶ C. H. Wang,³³ M. J. Wang,³³ A. Warburton,¹⁴ T. Watanabe,³⁷ T. Watts,³² R. Webb,³⁴ C. Wei,⁶ H. Wenzel,¹⁶ W. C. Wester, III,⁷ A. B. Wicklund,¹ E. Wicklund,⁷ R. Wilkinson,²⁶ H. H. Williams,²⁶ P. Wilson,⁵ B. L. Winer,²³ D. Winn,²⁰ D. Wolinski,²⁰ J. Wolinski,²¹ S. Worm,²² X. Wu,¹⁰ J. Wyss,²⁷ A. Yagil,⁷ W. Yao,¹⁸ K. Yasuoka,³⁷ G. P. Yeh,⁷ P. Yeh,³³ J. Yoh,⁷ C. Yosef,²¹ T. Yoshida,²⁴ I. Yu,⁷ A. Zanetti,³⁶ F. Zetti,²⁷ and S. Zucchelli²

(CDF Collaboration)

¹ Argonne National Laboratory, Argonne, Illinois 60439

² Istituto Nazionale di Fisica Nucleare, University of Bologna, I-40127 Bologna, Italy

³ Brandeis University, Waltham, Massachusetts 02254

⁴ University of California at Los Angeles, Los Angeles, California 90024

⁵ University of Chicago, Chicago, Illinois 60637

⁶ Duke University, Durham, North Carolina 27708

⁷ Fermi National Accelerator Laboratory, Batavia, Illinois 60510

⁸ University of Florida, Gainesville, FL 32611

⁹ Laboratori Nazionali di Frascati, Istituto Nazionale di Fisica Nucleare, I-00044 Frascati, Italy

¹⁰ University of Geneva, CH-1211 Geneva 4, Switzerland

¹¹ Harvard University, Cambridge, Massachusetts 02138

¹² Hiroshima University, Higashi-Hiroshima 724, Japan
¹³ University of Illinois, Urbana, Illinois 61801
¹⁴ Institute of Particle Physics, McGill University, Montreal H3A 2T8, and University of Toronto,
 Toronto M5S 1A7, Canada
¹⁵ The Johns Hopkins University, Baltimore, Maryland 21218
¹⁶ Institut für Experimentelle Kernphysik, Universität Karlsruhe, 76128 Karlsruhe, Germany
¹⁷ National Laboratory for High Energy Physics (KEK), Tsukuba, Ibaraki 305, Japan
¹⁸ Ernest Orlando Lawrence Berkeley National Laboratory, Berkeley, California 94720
¹⁹ Massachusetts Institute of Technology, Cambridge, Massachusetts 02139
²⁰ University of Michigan, Ann Arbor, Michigan 48109
²¹ Michigan State University, East Lansing, Michigan 48824
²² University of New Mexico, Albuquerque, New Mexico 87131
²³ The Ohio State University, Columbus, OH 43210
²⁴ Osaka City University, Osaka 588, Japan
²⁵ Universita di Padova, Istituto Nazionale di Fisica Nucleare, Sezione di Padova, I-36132 Padova, Italy
²⁶ University of Pennsylvania, Philadelphia, Pennsylvania 19104
²⁷ Istituto Nazionale di Fisica Nucleare, University and Scuola Normale Superiore of Pisa, I-56100 Pisa, Italy
²⁸ University of Pittsburgh, Pittsburgh, Pennsylvania 15260
²⁹ Purdue University, West Lafayette, Indiana 47907
³⁰ University of Rochester, Rochester, New York 14627
³¹ Rockefeller University, New York, New York 10021
³² Rutgers University, Piscataway, New Jersey 08855
³³ Academia Sinica, Taipei, Taiwan 11530, Republic of China
³⁴ Texas A&M University, College Station, Texas 77843
³⁵ Texas Tech University, Lubbock, Texas 79409
³⁶ Istituto Nazionale di Fisica Nucleare, University of Trieste/ Udine, Italy
³⁷ University of Tsukuba, Tsukuba, Ibaraki 315, Japan
³⁸ Tufts University, Medford, Massachusetts 02155
³⁹ Waseda University, Tokyo 169, Japan
⁴⁰ University of Wisconsin, Madison, Wisconsin 53706
⁴¹ Yale University, New Haven, Connecticut 06520

Abstract

We observe hadronic W decays in $t\bar{t} \rightarrow W(\rightarrow \ell\nu) + \geq 4$ jet events using a 109 pb^{-1} data sample of $p\bar{p}$ collisions at $\sqrt{s} = 1.8 \text{ TeV}$ collected with the Collider Detector at Fermilab (CDF). A peak in the dijet invariant mass distribution is obtained that is consistent with W decay and inconsistent with the background prediction by 3.3σ . From this peak we measure the W mass to be $77.2 \pm 4.6 \text{ (stat+syst) GeV}/c^2$. This result demonstrates the presence of two W bosons in $t\bar{t}$ candidates in the $W(\rightarrow \ell\nu) + \geq 4$ jet channel.

PACS numbers: 14.65.Ha, 13.38.Be

CDF presented the first direct evidence for top quark production with 19.3 pb^{-1} of data collected in 1992-93 [1] and also reported a detailed kinematic study of top decays with this data sample [2]. In 1994-95, the existence of the top quark was firmly established by CDF [3] and D \emptyset [4]. CDF observed and studied $t\bar{t}$ production using a sample of 67 pb^{-1} employing techniques similar to those previously published [5, 6].

In the Standard Model, a top quark decays predominantly into a bottom quark and a W boson. As a part of the CDF kinematic studies of $t\bar{t}$ production and decay, we have searched for hadronic W decays in a $t\bar{t}$ -enriched sample containing a high- P_T lepton and four or more jets, which is consistent with the process $p\bar{p} \rightarrow t\bar{t}X \rightarrow W^+bW^-\bar{b}X \rightarrow \ell\nu bjj\bar{b}X$ with $\ell = e$ or μ , and j representing a jet. Hereafter we call these events “ $W+ \geq 4$ jet events”. The observation of hadronic W decays in $W+ \geq 4$ jet events demonstrates the presence of two W bosons in the final state for $t\bar{t}$ candidates.

The studies reported here use a $109 \pm 7 \text{ pb}^{-1}$ data sample. Three analysis techniques yield signal-to-background ratios ranging from 0.23 to 1.4 in the dijet invariant mass region $60\text{-}100 \text{ GeV}/c^2$.

The CDF detector consists of a magnetic spectrometer surrounded by calorimeters and muon chambers [7]. A silicon vertex detector (SVX), located immediately outside the beampipe, provides precise track reconstruction in the plane transverse to the beam and is used to identify secondary vertices from b and c quark decays [8]. The momenta of charged particles are measured in the central tracking chamber (CTC) which is in a 1.4 T superconducting solenoidal magnet. Outside the CTC, electromagnetic and hadronic calorimeters cover the pseudorapidity [9] region $|\eta| < 4.2$ and are used to identify jets and electron candidates. Outside the calorimeters, drift chambers in the region $|\eta| < 1.0$ provide muon identification.

To select $t\bar{t} \rightarrow W+ \geq 4$ jet candidates, we require an isolated, high- P_T electron or muon ($P_T > 20 \text{ GeV}/c$), high missing transverse energy [9] ($\cancel{E}_T > 20 \text{ GeV}$), three jets with $E_T > 15 \text{ GeV}$ and $|\eta| < 2.0$, and a fourth jet with $E_T > 8 \text{ GeV}$ and $|\eta| < 2.4$. After these cuts 163 events remain. The expected fraction of $t\bar{t}$ events in this sample is 33%. The fraction was determined by extrapolating the background calculation performed on the $W+ \geq 3$ jet sample for the $t\bar{t}$ cross section measurement [10] to include the additional requirement of a fourth jet.

For the event selection, neither the jet E_T nor the \cancel{E}_T are corrected for detector effects. However, when calculating a dijet invariant mass, jet energies are corrected by a pseudorapidity and energy-dependent factor which accounts for such effects as calorimeter nonlinearity, reduced response at detector boundaries, contributions from the underlying event and multiple interactions and losses outside the clustering cone [11]. We apply an additional energy correction to the four highest- E_T jets in a $t\bar{t}$ candidate event. The correction depends on the type of parton they are assigned to: a light quark, a hadronically decaying b quark, or a b quark that decayed semileptonically [1]. This parton-specific correction was derived from a study of $t\bar{t}$ events generated with the HERWIG Monte Carlo program [12]. This correction is applied in order to reconstruct the original parton energy as closely as possible. These cuts and corrections are the same as those used in the top

mass measurement [1] before requiring a b jet.

Monte Carlo $t\bar{t}$ events are generated by the HERWIG program [12] with a top mass of 175 GeV/c^2 [13]. The expected background from direct $W +$ jets production is estimated using the VECBOS Monte Carlo calculation [14] to generate $W + 3$ parton matrix elements. To model $W + \geq 4$ jet events we implement a simulation of parton fragmentation with a shower algorithm based on HERWIG. The lowest-order matrix elements are sensitive to the choice of the mass scale in the strong coupling constant α_s . We use two Q^2 scales, namely, the square of the average jet P_T ($\langle P_T \rangle^2$) and the square of the W boson mass (M_W^2). We use $\langle P_T \rangle^2$ as a standard Q^2 scale and M_W^2 for an estimate of the systematic uncertainty. A more detailed description of the Monte Carlo samples can be found elsewhere [1].

The lepton- \cancel{E}_T transverse mass distribution is shown in Figure 1. Also shown are the Monte Carlo expectations from $t\bar{t}$ as well as $t\bar{t}$ plus QCD $W +$ jets background. The Monte Carlo expectations are normalized to the number of events observed.

We use three methods to search for W decay to two jets: a top mass reconstruction technique, a total transverse energy cut, and the identification of both b jets.

In the first method, we search for a W decaying to two jets by kinematically reconstructing $t\bar{t} \rightarrow \ell\nu b j j \bar{b}$ with a constrained fitting technique similar to the one used for the determination of the top mass [1]. The constraints used in the top mass measurement include the requirement that the two jets hypothesized to come from the W decay have an invariant mass equal to the W mass. Here we eliminate the W mass constraint. There are multiple solutions due to the ambiguity in determining the neutrino longitudinal momentum and the assignment of jets to the parent partons. We choose the solution with the lowest χ^2 . The resolution and signal-to-background ratio for $t\bar{t}$ events is improved by requiring a b -tag in the event and requiring that the tagged jet correspond to a b jet in the fit. To tag b jets, we exploit either the long lifetime of b quarks by requiring a secondary vertex (SVX b -tag), or the semileptonic decays of b quarks by searching for additional leptons (SLT b -tag) [1]. The fraction of correct W jet assignments was found from Monte Carlo studies to be improved from 22% before b -tagging to 37% after tagging.

Of the 163 events passing the $W + \geq 4$ jet selection cuts, 37 have at least one b -tag found by the SVX or SLT algorithms. The expected background is $8.9^{+2.0}_{-1.7}$ events, calculated using techniques described in [10]. The dijet invariant mass distribution for these events is shown in Figure 2. Also shown are the Monte Carlo distributions for $t\bar{t}$ and background, normalized to 28.1 and 8.9 events respectively. We note a strong enhancement in the data distribution near the world-average W mass [15].

The second method employs a cut on the minimum total transverse energy H_T to enhance the $t\bar{t}$ contribution in the sample. H_T is defined as the scalar sum of the P_T of the lepton (E_T for an electron), the four highest- E_T jets, and the \cancel{E}_T [6]. We optimize the H_T threshold (310 GeV) using $t\bar{t}$ and background simulations. This cut improves the fraction of $t\bar{t}$ events in the sample from 33% to 55%.

We calculate the invariant mass of each two-jet pair out of the four highest- E_T jets. Monte Carlo simulations predict that two jets from W decay are included in the four highest- E_T jets with an efficiency of 66%. There are six combinations of two jets in

each event. To determine the contributions from non- $t\bar{t}$ backgrounds and combinatoric backgrounds in $t\bar{t}$ events, we fit the dijet mass distribution M_{jj} outside the W mass region to the following function: $N_{bg}f_{bg}(M_{jj}) + N_{comb}f_{comb}(M_{jj})$, where N_{bg} and N_{comb} are the number of non- $t\bar{t}$ and $t\bar{t}$ combinatoric background dijet pairs respectively, and f_{bg} and f_{comb} are their dijet mass distributions, derived from Monte Carlo. Since non- $t\bar{t}$ backgrounds, such as WW , WZ , and $b\bar{b}$ are smaller and give dijet mass distributions similar to QCD $W +$ jets, f_{bg} is obtained from VECBOS calculation of QCD $W +$ jets background.

We extract the $W \rightarrow 2$ jets signal by subtracting the QCD $W +$ jets background and the combinatoric background as shown in Figure 3. For the $W + \geq 4$ jet sample of $t\bar{t}$ production, the reconstructed mass peak of the W decaying into dijets is well described by a Gaussian distribution with a standard deviation of $11.7 \text{ GeV}/c^2$. We fit this distribution to a Gaussian function with a fixed width and obtain 29 ± 13 $W \rightarrow 2$ jet events in the mass region $70\text{-}90 \text{ GeV}/c^2$, which is consistent with the number of $W \rightarrow 2$ jet events (20 ± 6) expected from the CDF $t\bar{t}$ production cross section measurement [10]. This excess is inconsistent with the expected background by 2.8σ , corresponding to a probability of 2.6×10^{-3} of it being a background fluctuation. The signal-to-background ratio in the mass region $60\text{-}100 \text{ GeV}/c^2$ is 0.23, and the overall fraction of non- $t\bar{t}$ background is $(27 \pm 14)\%$. The dijet invariant mass peak has a mean of $77.1 \pm 3.8(\text{stat}) \pm 3.6(\text{syst}) \text{ GeV}/c^2$. The systematic uncertainty comes mainly from the jet energy scale, which is the uncertainty on how well our measured jet energies correspond to the original parton energies. The systematics are listed in Table 1, and are described in more detail in Ref. [13].

In the third method, we isolate the hadronic W decay by identifying two b jets in the four highest- E_T jets of $W + \geq 4$ jet events. Such events are hereafter called “double b -tagged” $W + \geq 4$ jet events. Double b -tagging eliminates ambiguity about which two jets are assigned to the W , and further suppresses non- $t\bar{t}$ background. Once we find at least one b jet with an SVX tag or an SLT tag in an event, we look for the second b jet. The second b -tag can be an SVX tag, an SLT tag or a Jet Probability tag [16]. The Jet Probability algorithm obtains the probability that a jet is consistent with the decay of a zero-lifetime particle by using the impact parameters of the tracks in the jet as measured in the silicon vertex detector. Jets with probabilities less than 5% are considered tagged. We form the invariant mass of the remaining two untagged jets.

In our HERWIG $t\bar{t}$ Monte Carlo sample, 25% of the events are double b -tagged. The technique finds the two correct W jets in 43% of these events. However, this number is sensitive to the amount of initial and final state radiation in the simulation, since the largest contamination (38% of double b -tagged events) comes from events where the four highest- E_T jets do not correspond to two b jets and two jets from W decay. Other $t\bar{t}$ backgrounds include events where both W bosons decayed leptonically and only one lepton was identified (8%), events where a c quark from W decay was tagged (8%), and mistags in jets from W decay (3%), where a mistag means a tag of a jet originating from neither a b nor a c quark.

We expect 1.3 ± 0.3 double-tagged events from non- $t\bar{t}$ background, with the largest contributions being 0.6 ± 0.2 events from mistags and 0.4 ± 0.2 events from $Wb\bar{b}$ and $Wc\bar{c}$ processes which are QCD $W +$ jets events containing real heavy flavor.

In the data, we find eleven double b -tagged events. The dijet invariant mass of the two untagged jets in these eleven events is shown in Figure 4. Eight of the eleven dijet combinations fall in the mass window of $60\text{--}100\text{ GeV}/c^2$. In Monte Carlo simulations of both QCD $W + \text{jets}$ and $t\bar{t}$ backgrounds, only about a third of the dijet mass combinations fall in this window. The inset plot in Figure 4 shows the mass of the hadronic W candidates against the transverse mass of the leptonic W candidates in the same events.

We fit this mass distribution to a sum of a Gaussian $W \rightarrow 2$ jets signal, $t\bar{t}$ backgrounds, and non- $t\bar{t}$ backgrounds, and obtain a W mass of $78.1 \pm 4.4(\text{stat}) \pm 2.9(\text{syst})\text{ GeV}/c^2$, with the systematic uncertainties listed in Table 1. The fitted W signal has 8.7 events, and 0.7 events from $t\bar{t}$ backgrounds. Constraining the fit to the expected $W \rightarrow 2$ jets fraction in $t\bar{t}$ events yields 6.4 W events, and a W mass of $78.3 \pm 5.1(\text{stat}) \pm 2.9(\text{syst})\text{ GeV}/c^2$. We use this value for obtaining a final combined W mass.

We use likelihood fits to evaluate the significance of this peak. We first fit the data using a Gaussian W signal whose mean is the world-average W mass plus $t\bar{t}$ and non- $t\bar{t}$ backgrounds. Next we remove the signal term and note the change in likelihood. We then repeat this procedure on Monte Carlo pseudo-experiments using only $t\bar{t}$ and non- $t\bar{t}$ background events, and study how often the likelihood changes by at least the amount seen in the data. This change in likelihood was seen with a probability of 1.7×10^{-3} , corresponding to a Gaussian significance of 2.9σ . If we construct the pseudo-experiments with the expected W signal fraction, we find that a change in likelihood larger than the one seen in the data occurs 15% of the time.

Uncertainty (GeV/c^2)	H_T cut	double b -tag	common	combined
Statistical	4.6	5.1	-	3.5
Jet energy scale				2.8
(a) Detector effects	1.9	1.9	1.9	
(b) Soft gluon effects	2.0	2.0	2.0	
Other systematics				0.6
(a) Backgrounds	0.5	0.2	-	
(b) Fitting	1.9	0.6	-	
(c) H_T cut	1.0	-	-	
Total uncertainty	5.8	5.9	2.8	4.6

Table 1: The list of uncertainties (in GeV/c^2) in the $W \rightarrow 2$ jets mass for the H_T cut and double b -tag analyses. The columns “common” and “combined” correspond to the uncertainties common in the two analyses and the combined uncertainties of the two analyses, respectively.

An overall result is obtained by excluding the eleven double b -tagged events from the H_T cut analysis. We then combine the two analyses to obtain a W mass peak significance

of 3.3σ , corresponding to a probability of 5.4×10^{-4} of it being a background fluctuation and a W mass of $77.2 \pm 3.5(\text{stat}) \pm 2.9(\text{syst})$ GeV/c^2 with the systematic uncertainties listed in Table 1. This is consistent with the current world-average W mass of 80.375 ± 0.120 GeV/c^2 [15].

In conclusion, we observe hadronic W decays as a dijet mass peak in $t\bar{t} \rightarrow W+ \geq 4$ jet events. This demonstrates the presence of two W bosons in the $t\bar{t}$ candidates. In the future, these techniques can be used to set limits on nonstandard top decays.

We thank the Fermilab staff and the technical staffs of the participating institutions for their contributions. This work was supported by the U.S. Department of Energy and the National Science Foundation; the Italian Istituto Nazionale di Fisica Nucleare; the Ministry of Science, Culture, and Education of Japan; the Natural Sciences and Engineering Research Council of Canada; the National Science Council of the Republic of China and the A. P. Sloan Foundation.

References

- [1] F. Abe *et al.*, Phys. Rev. Lett. **73**, 225 (1994), hep-ex/9405005; F. Abe *et al.*, Phys. Rev. **D 50**, 2966 (1994).
- [2] F. Abe *et al.*, Phys. Rev. **D 51**, 4623 (1995), hep-ex/9412009.
- [3] F. Abe *et al.*, Phys. Rev. Lett. **74**, 2626 (1995), hep-ex/9503002.
- [4] S. Abachi *et al.*, Phys. Rev. Lett. **74**, 2632 (1995), hep-ex/9503003.
- [5] F. Abe *et al.*, Phys. Rev. **D 52**, R2605 (1995).
- [6] F. Abe *et al.*, Phys. Rev. Lett. **75**, 3997 (1995), hep-ex/9506006.
- [7] F. Abe *et al.*, Nucl. Instrum. Methods Phys. Res., Sect. **A 271**, 387 (1988).
- [8] S. Cihangir *et al.*, Nucl. Instrum. Methods Phys. Res., Sect. **A 360**, 137 (1995). Our previous silicon vertex detector is described in D. Amidei *et al.*, Nucl. Instrum. Methods Phys. Res., Sect. **A 350**, 73 (1994).
- [9] In the CDF coordinate system, θ is the polar angle with respect to the proton beam direction. The pseudorapidity η is defined as $-\ln \tan(\theta/2)$. The transverse momentum of a particle is $P_T = P \sin \theta$. The analogous quantity using calorimeter energies, $E_T = E \sin \theta$, is called transverse energy. Missing transverse energy \cancel{E}_T is defined as $-\sum E_T^i \cdot \hat{n}_i$, where \hat{n}_i are the unit vectors, in the plane transverse to the beam line, pointing from the interaction point to the energy deposition in cell i of the calorimeter.
- [10] F. Abe *et al.*, FERMILAB-PUB-97/286-E, hep-ex/9710008.
- [11] F. Abe *et al.*, Phys. Rev. **D 45**, 1448 (1992); F. Abe *et al.*, Phys. Rev. **D 47**, 4857 (1993).

- [12] G. Marchesini and B. R. Webber, Nucl. Phys. **B 310**, 461 (1988); G. Marchesini *et al.*, Comput. Phys. Comm. **67**, 465 (1992).
- [13] F. Abe *et al.*, FERMILAB-PUB-97/284-E.
- [14] F. A. Berends, W. T. Giele, H. Kuif, B. Tausk, Nucl. Phys. **B 357**, 32 (1991); W. Giele, Ph. D. Thesis, Leiden (1989).
- [15] M. Lancaster, Proceedings of de la Vallée d'Aoste, La Thuile, 1997; ed. M. Greco.
- [16] D. Buskulic *et al.*, Phys. Lett. **B 313**, 535 (1993).

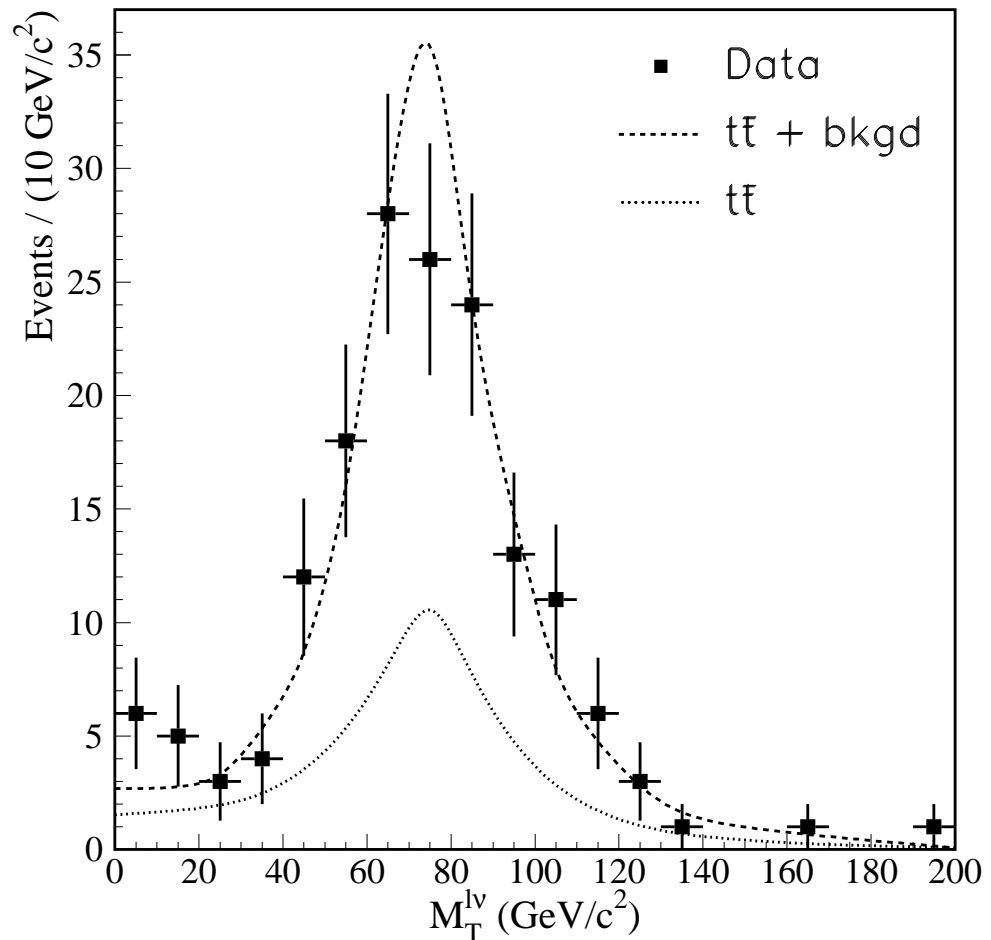


Figure 1: The lepton- \cancel{E}_T (neutrino) transverse mass distribution in the $W + \geq 4$ jet data (points) along with the Monte Carlo expectations from $t\bar{t}$ (dotted) and $t\bar{t}$ plus QCD W + jets background (dashed).

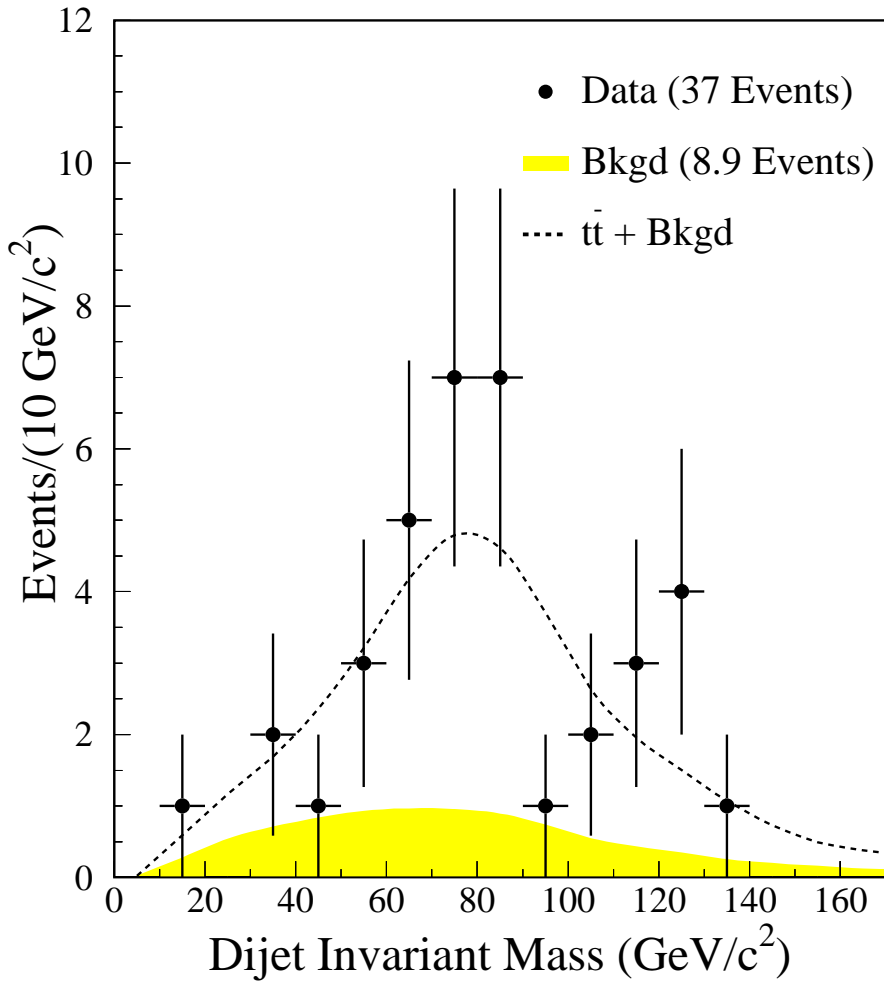


Figure 2: Invariant mass distribution for the two jets that are associated with the W by the constrained kinematic fit. The shaded histogram shows the expected distribution from background events; $t\bar{t}$ plus background events are shown as a dashed line.

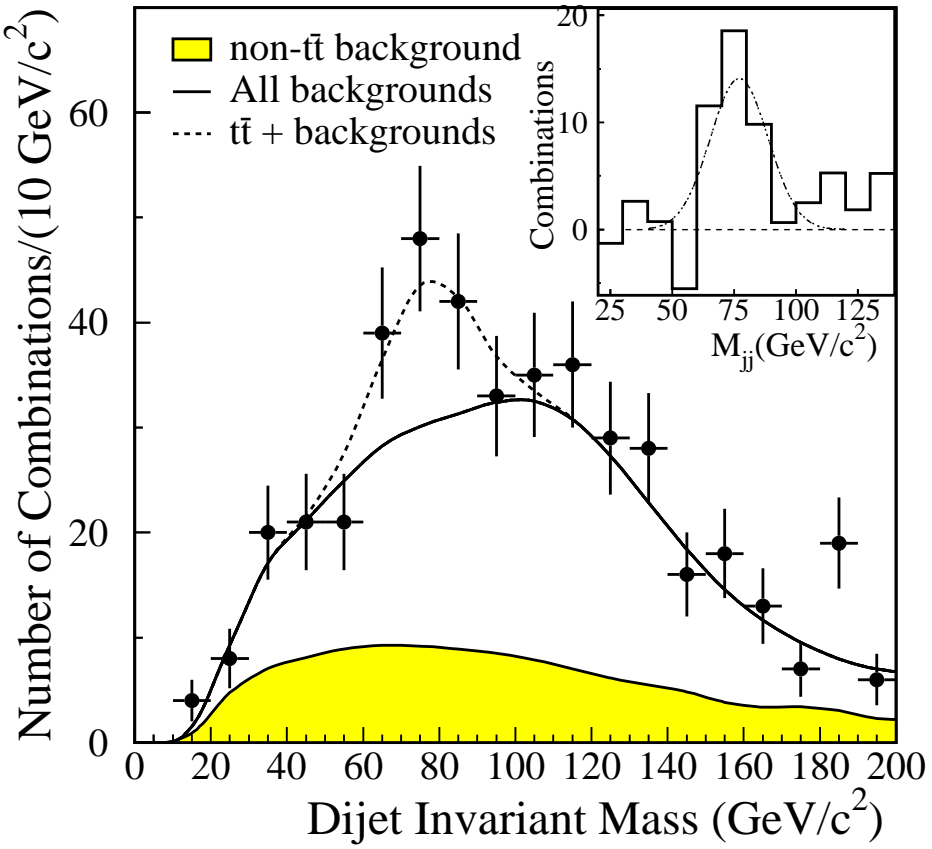


Figure 3: Dijet mass distribution in $W + \geq 4$ jet events after the $H_T > 310 \text{ GeV}$ cut. Also shown are a fitted curve of the sum (solid) of the VECBOS $W +$ jets background (shaded) and the combinatoric background from $t\bar{t}$ events. A Gaussian distribution fitted to the W mass peak is shown by the dotted curve. The inset shows the W mass peak after subtracting the backgrounds.

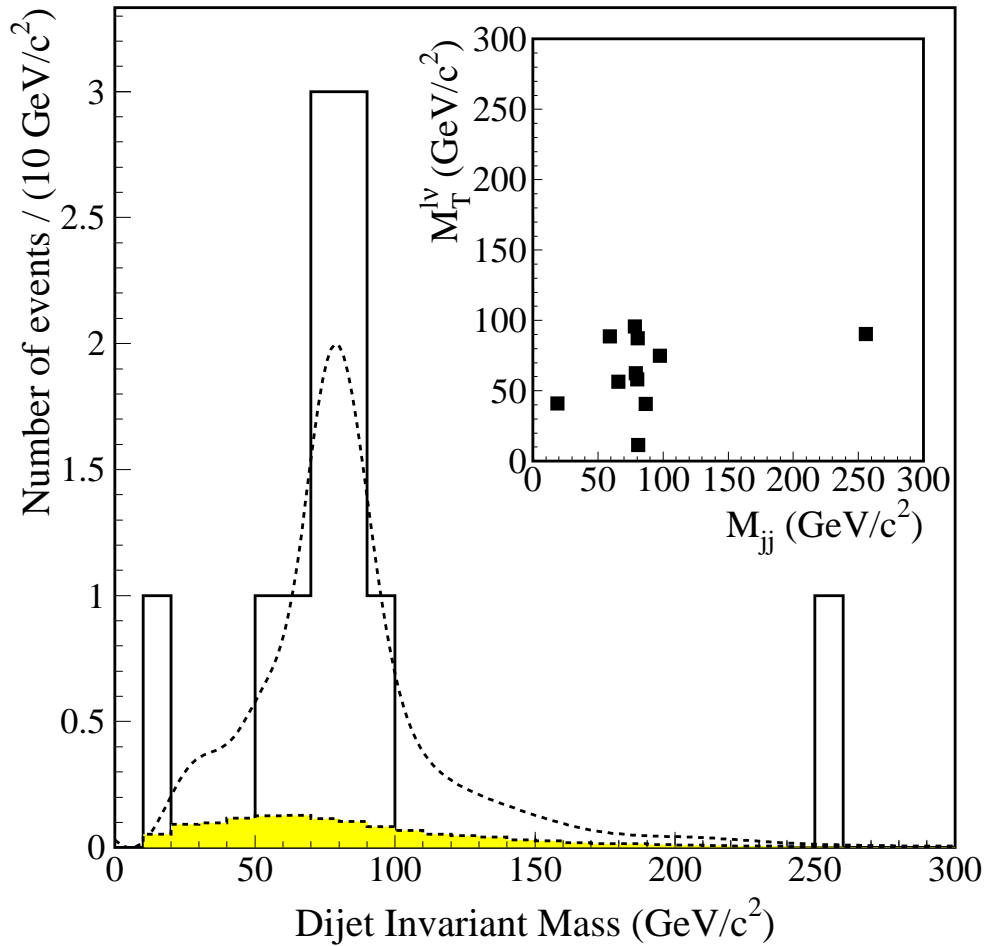


Figure 4: Dijet mass spectrum of the two untagged jets in double b -tagged events. The shaded curve shows the expected distribution from QCD $W + \text{jets}$ background and the dashed curve is from $t\bar{t}$ plus background. The inset compares the lepton- \cancel{E}_T (neutrino) transverse mass to the dijet invariant mass in these eleven events showing evidence for events with both a leptonically-decaying W and a hadronically-decaying W .